

Unsteady MHD Heat Mass Transfer Couette Flow in a Free Convective Vertical Channel due to Dufour and Buoyancy Distribution Effects

¹B. Y. Isah and ²F. Abdullah

¹Department of Mathematics Usmanu Danfodiyo University, Sokoto P.M.B.2346, Sokoto State

²Department of Mathematics Waziri Ummaru Federal Polytechnic BirninKebbi, Kebbi State

Corresponding author's E-Mail: isah.bala@udusok.edu.ng

Article Information

Article history:

Received 14 September 2021

Revised 28 October 2021

Accepted 22 November 2021

Available online 30 Dec. 2021

Keywords: MHD,
Dufour effect,
Buoyancy distribution effect, Heat
Mass Transfer



<https://doi.org/10.37933/nipes.e/3.4.2021.12>

<https://nipesjournals.org.ng>
© 2021 NIPES Pub. All rights reserved

Abstract

This study investigates the effects of Dufour on unsteady heat and mass transfer Couette flow in free convective vertical channels in the presence of buoyancy distribution effects due to ramped and isothermal temperature. Fitting dimensional quantities were used to convert the coupled non-linear dimensional partial differential equations of the flow into non-dimensional non-linear partial differential equations. Finite element method (FEM) was employed to solve the non-linear time dependent momentum, energy and concentration equations under appropriate initial and boundary conditions. The expressions of velocity, temperature, concentration, skin friction; Nusselt number as well as Sherwood number subject to isothermal and ramped temperature boundary conditions were gained. Selected set of graphical results illustrate that the thermo—physical parameters control the flow and are in good agreement with the previous literatures. From the outcome of the results, it was noticed that increasing the porosity parameter K , ratio of mass transfer parameter N , buoyancy effect term parameter r_1 , Eckert number Ec and Dufour number Df intensifies the velocity profiles while reverse is the case with the increase of magnetic parameter M and Prandtl number Pr . Similarly increasing the porosity parameter K , ratio of mass transfer parameter N , buoyancy effect term parameter r_1 , enhances the temperature profile and reverse is the case with the increase of, Prandtl number Pr . Also concentration profiles get enhanced with the increase of Schmidt Sc number. The skin friction at both $y = 0$ and $y = 1$ gets intensified with the increase Dufour number Df and buoyancy parameter r_1 for both ramped and isothermal temperature.

1. Introduction

In most real-world practical settings such as condensation, evaporation and chemical reactions the heat transfer process is mostly complemented by the mass transfer activity. This is attributed to its usefulness in understanding number of technical transfer processes mostly found in chemically processed industries such as polymer and food processing Siva *et al.* [1]. The heat transfer produced by concentration gradients is called Dufour effect. Dufour effect was discovered in 1873 by

Physicist called Dufour and he was correspondingly referred the Dufour. Shankar and Rajashekar [2] investigated on the effects of viscous dissipation and diffusion thermo on an unsteady MHD flow with an inclined oscillating plate started impulsively and found that, the velocity get reduced with increase in Dufour number and phase angle. The temperature profiles rise with the increase in Dufour number, Prandtl number and Schmidt number. Similarly, Rajakumar *et al.* [3] investigated Dufour effects, radiation absorption, chemical reaction, and viscous dissipation effects on unsteady magneto hydrodynamic free convective Casson fluid flow through a semi-infinite vertical oscillatory porous plate of time dependent permeability with hall and ion-slip current in a rotating system and found that as the Dufour effect parameter increases the velocity and temperature get enhanced.

The effects diffusion thermo and thermo diffusion on unsteady MHD natural convection heat and mass transfer flow past an accelerated vertical porous plate in the presence of thermal radiation, variable temperature and also variable concentration were investigated by Chandra and Raju [4] and discovered that, the fluid velocity enhances with the increasing values of Soret number and Dufour number. The temperature of the fluid enhances with the increase of Soret and Dufour effects. Also increasing values of Soret number results in rising of the concentration, but it falls down under the influence of Schmidt number and Dufour number. Skin friction gets reduced for increasing values of both Soret and Dufour numbers. Similarly, Reddy *et al.* [5] studied the heat absorption, thermal-diffusion and diffusion- thermo effects on unsteady viscous incompressible MHD flow along semi-infinite inclined permeable moving plate with variable temperature and mass diffusion embedded in a porous medium and found that, an increase in the Dufour number enhances thermal boundary layer and the velocity increases with the increase in Dufour number, Soret number, Grashof number and solutal Grashof number. Similarly, skin-friction and nusselt get enlarged when Dufour number and Soret number increase, while Sherwood number falls as Dufour number and Soret number increase. Bilal *et al.* [6] analyzed the effect of mixed convection flow of an Oldroyd-B fluid is investigated in the presence of convective boundary condition and Soret and Dufour effects. Emmanuel *et al.* [7] investigated the effect of thermal diffusion and diffusion thermo on heat and mass transfer over a vertical porous surface with convective heat transfer and found that combined effects of thermal diffusion and diffusion thermo and the other embedded parameters can help control flow kinematics and enhances both the heat and mass transfer process. Also Sasikumar and Govindarajan [8] studied the Soret effects on MHD Oscillatory flow with heat source in presence chemical reaction in an asymmetric wavy channel filled with porous medium is carried out and discovered that fluid velocity increases with increase in Soret number. Similarly, Gbadeyan *et al.* [9] studied free convective heat and mass transfer of an incompressible electrically conducting fluid in a finitely long vertical wavy channel, considering Soret, Dufour and chemical reaction effects in the presence of constant heat source or sink and concluded that mean velocity and temperature get reduced with increase in Dufour number and Soret number. Additionally, Idowu and Falodun [10] analyzed the effects of Soret and Dufour on MHD heat and mass transfer of a viscoelastic fluid pass over a semi-infinite vertical plate and concluded that fluid velocity and temperatures increased with increase in Dufour parameter. Also increase in Soret number leads to increase of fluid velocity and concentration

Reddy *et al.* [11] studied the influence of an unsteady magnetohydrodynamic natural convection on the Couette flow of electrically conducting water at 4°C ($\text{Pr} = 11.40$) in a rotating system. The primary velocity, secondary velocity and temperature of water at 4°C as well as shear stresses and rate of heat transfer have been obtained for both ramped temperature and isothermal plates and it was found that The primary velocity of the fluid increases with the increase of Gr and decreases with the increase of M^2 , Ω^2 and Pr . The secondary velocity of the fluid increases with the increase of Gr and decreases with the increase of M^2 and Pr .

Additionally, Shagaiya and Daniel [12] investigated the theoretical influence of buoyancy and thermal radiation on MHD flow over a stretching porous sheet. It was found that when the buoyancy parameter is increase the fluid velocity increases. The hydrodynamic boundary layer and thermal boundary layer thickness increase as a result of increase in radiation. Shagaiya and Simon [13] analyzed influence of buoyancy and thermal radiation on MHD flow over a stretching porous sheet and found that when the buoyancy parameter increases, the fluid velocity increases and the thermal boundary layer decreases. Adamu and Bandari [14] studied the effect of thermal and solutal buoyancy parameters on the nanofluid flow heat and mass transfer characteristics due to a stretching sheet in the presence of a magnetic field and discovered that The axial velocity of the fluid increases with an increase of both thermal and solutal buoyancy parameter while the thermal conductivity of the fluid decreases

Prabhakar [15] analyzed the effects viscous dissipation on unsteady heat and mass transfer free convection past an infinite vertical porous plate under the influence of a uniform magnetic field. The present research study adopted and extended the Prabhakar model by incorporating diffusion-thermo effects and buoyancy distribution effects on unsteady heat and mass transfer Couette flow in free convective vertical channels due to ramped and isothermal temperature. Finite element method was employed to solve the governing coupled non-linear differential equations. The expression of velocity temperature and concentration as well as shear stress have been obtained for both and continuous ramped temperature isothermal plates

2. Formulation of the Problem

Consider an unsteady free convective flow of an incompressible electrically conducting viscous dissipative fluid in finite vertical plates.

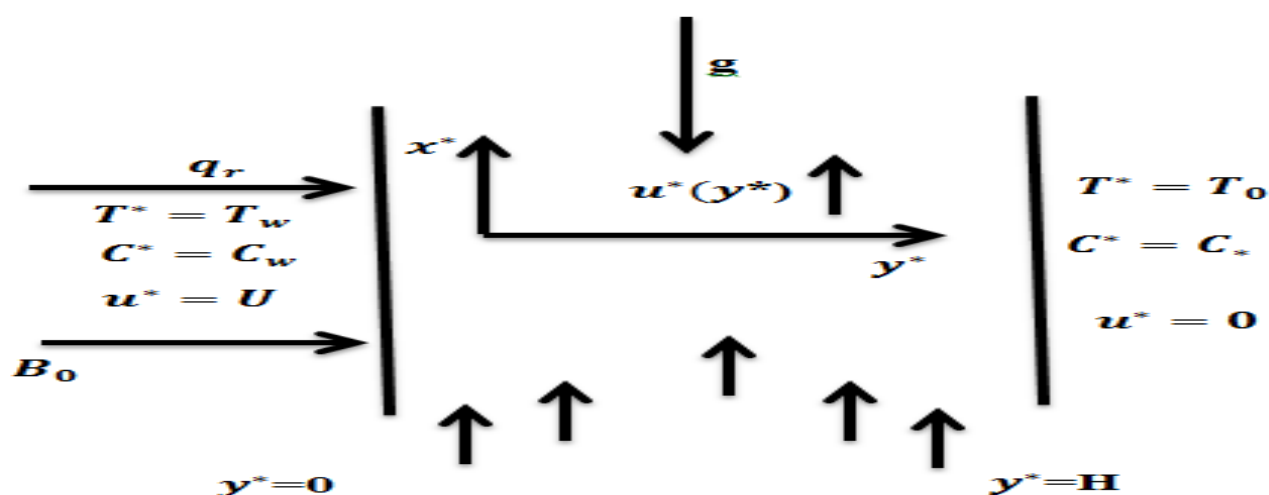


Figure 1: Geometry of the Problem

Let the x^* -axis be chosen along the plate in the vertically upward direction and the y^* axis is chosen normal to the plate. A uniform magnetic field of intensity H_0 is applied transversely to the plate. The induced magnetic field is neglected as the magnetic Reynolds number of the flow is taken to be very small. Initially, the temperature of the plate T^* and the fluid T_w^* are assumed to be the same. The concentration of species at the plate C_w^* and C_0^* are assumed to be the same. At time $t^* > 0$, the plate temperature is changed to T_w^* , which is then maintained constant, causing convection currents to flow near the plate and mass is supplied at a constant rate to the plate. Under these conditions the

flow variables are functions of time t^* and space (channel width) y^* alone. By employing the Boussinesq approximation, the governing equations describing momentum, energy and mass transfer equations in the presence Soret effect, and other controlling parameters of the three problems take the following form:

Momentum equation

$$\frac{\partial u^*}{\partial t^*} = \frac{\partial^2 u^*}{\partial y^{*2}} + g\beta(T^* - T_w^*) - g\beta^*(C^* - C_0) - \frac{\sigma\mu_e^2 H_0^2 u^*}{\rho} - \frac{vu^*}{K^*} \quad (1)$$

Heat Transfer equation

$$\rho C_p \frac{\partial \theta^*}{\partial t^*} = k \frac{\partial^2 \theta^*}{\partial y^{*2}} + \mu \left[\frac{\partial u^*}{\partial y^*} \right]^2 + \frac{D_m \partial^2 C^*}{\alpha \partial y^{*2}} \quad (2)$$

Mass Transfer equation

$$\frac{\partial C^*}{\partial t^*} = \frac{\partial^2 C^*}{\partial y^{*2}} \quad (3)$$

The corresponding initial and boundary conditions are:

Case I: Isothermal Temperature

Case II: Continuous Ramped Temperature

$$\left. \begin{aligned} & t^* \leq 0, u^* = 0, T^* = T_0 \text{ for all } 0 \leq y^* \leq L \\ & t^* > 0 \left\{ \begin{aligned} & u^* = u, T^* = T_w, C^* = C_w^* \text{ at } y^* = 0 \\ & u^* = 0, T^* = r_t^* T, C^* = C_w^* \text{ at } y^* = L \end{aligned} \right. \end{aligned} \right\}, \left. \begin{aligned} & t^* \leq 0, u^* = 0, T^* = T_0 \text{ for all } 0 \leq y^* \leq L \\ & t^* > 0 \left\{ \begin{aligned} & u^* = u, T^* = T_0 + \frac{(T_w^* - T_0)t^*}{T_R}, C^* = C_w^* \text{ at } y^* = 0 \\ & u^* = 0, T^* = r_t^* T, C^* = C_w^* \text{ at } y^* = L \end{aligned} \right. \end{aligned} \right\}$$

(4)

The non- dimensional quantities introduced in the above equations are defined as:

$$\left. \begin{aligned} U_0 &= (vgbDT)^{1/3}, \quad L = \left(\frac{g b D T}{v^2} \right)^{-1/3}, \quad T_R = \frac{(g b D T)^{-2/3}}{v^{-1/3}} \\ DT &= T_w^* - T_0^*, \quad t = \frac{t^*}{T_R}, \quad y = \frac{y^*}{L}, \quad r_t = \frac{r_t^* - T_0}{T_w^* - T_0} \\ u &= \frac{u^*}{U_0}, \quad K = \frac{K^*}{v T_R}, \quad q = \frac{T^* - T_0}{T_w^* - T_0}, \quad f = \frac{C^* - C_0}{C_w^* - C_0} \\ Pr &= \frac{m C_p}{k}, \quad Sc = \frac{v}{D_m}, \quad Ec = \frac{U_0^2}{C_p DT}, \quad Df = \frac{D_m (C_w - C_0)}{a (T_w - T_0)} \\ N &= \frac{b (C_w^* - C_\infty^*)}{b (T_w^* - T_0^*)}, \quad M = \frac{sm^2 H_0^2 T_R}{r} \end{aligned} \right\} \quad (5)$$

3. Method of the Solution

The method employed to solve the coupled non-linear system of partial differential equations was finite element method (Galerkin's approach) and the summarized fundamental steps of the method are as follows:

Step 1: Discretization of the Domain into Elements: This is the first and most important step in the Finite Element Method (FEM) as the basic concept of the FEM is to divide the structure or solution region into subdivisions called finite elements (Finite Element Mesh). In this step the number, type, size, and arrangement of the elements are to be decided.

Step 1: Derivation of Element Equations: Derivation of the element equations could be achieved through the following:

- i. A typical element is picked from the mesh and then you construct variational formulation of the problem over that element.
- ii. An approximating solution of the variational problem over that element is assumed, and by substituting it in the system, the element equations are generated. The function employed to represent the solution within each element is called shape, basic or interpolating function the function.
- iii. The element matrix, which is also known as the stiffness matrix is constructed by using the element interpolation functions.

Step 3: Assembly of Element Equations: Assemble element equations to obtain the overall elements equations. Since the structure is composed of several finite elements, the individual element stiffness matrices and load vectors are to be assembled in a suitable manner.

Step 4: Imposition of Boundary Conditions: The physical boundary conditions are imposed on the assembled equation appropriately.

Step 5: Solution to Assembled Equations: The assembled equations finally obtained can be solved by any of the numerical techniques such as the Gauss elimination method, LU decomposition method.

Now on the substitution of equations (5) into (1) - (4), the following governing equations in non-dimensional form are obtained.

$$\frac{\partial u}{\partial t} = \frac{\partial^2 u}{\partial y^2} + Grq + Nf - (M + \frac{1}{K})u$$

$$(6) Pr \frac{\partial \theta}{\partial t} = \frac{\partial^2 \theta}{\partial y^2} + Ec \left(\frac{\partial u}{\partial y} \right)^2 + Df \frac{\partial^2 C}{\partial^2 y^2}$$

(7)

$$Sc \frac{\partial C}{\partial t} = \frac{\partial^2 C}{\partial y^2}$$

(8)

Case I: Isothermal Temperature

$$\left. \begin{aligned} t \leq 0, u = 0, \theta = 0, \phi = 0 \text{ for all } y \\ \text{For } t \geq 0: \\ u = 1, \theta = 1, \phi = 1 \quad \text{at } y = 0 \\ u = 0, \theta = r_1, \phi = 0 \quad \text{at } y = 1 \end{aligned} \right\}$$

Case II: Continuous Ramped Temperature

$$\left. \begin{aligned} t \leq 0, u = 0, \theta = 0, \phi = 0 \text{ for all } y \\ \text{For } t \geq 0: \\ u = 1, \theta = t, \phi = 1 \quad \text{at } y = 0 \\ u = 0, \theta = r_1, \phi = 0 \quad \text{at } y = 1 \end{aligned} \right\}$$

(9)

Now (6) to be solved under the boundary conditions (9) using above mentioned method over the element

$$\int_{y_i}^{y_j} \left\{ N^T \left[\frac{\partial^2 u}{\partial y^2} - \frac{\partial u}{\partial t} - u \left(M + \frac{1}{K} \right) + Nf + q \right] \right\} dy = 0$$

(10)

Equation (3.5) is reduce to

$$\int_{y_i}^{y_j} \left\{ N^T \left[\frac{\partial^2 u}{\partial y^2} - \frac{\partial u}{\partial t} - M_1 u + P \right] \right\} dy = 0$$

(11)

Where $M_1 = M + \frac{1}{K}$ and $P = \theta + N\phi$

Applying integration by part to equation (11) yield;

$$\left[N^T \frac{\partial u}{\partial y} \right]_{y_i}^{y_j} - \int_{y_i}^{y_j} \frac{\partial N^T}{\partial y} \frac{\partial u}{\partial y} dy - \int_{y_i}^{y_j} N^T \frac{\partial u}{\partial t} dy - M_1 \int_{y_i}^{y_j} N^T u dy + P \int_{y_i}^{y_j} N^T dy = 0$$

(12)

Dropping the first term of equation (12)

$$\int_{y_i}^{y_j} \frac{\partial N^T}{\partial y} \frac{\partial u}{\partial y} dy + \int_{y_i}^{y_j} N^T \frac{\partial u}{\partial t} dy + M_1 \int_{y_i}^{y_j} N^T u dy - P \int_{y_i}^{y_j} N^T dy = 0$$

(13)

Let $u^{(e)} = u_i N_i + u_j N_j \Rightarrow u^{(e)} = [N][u]^T$ be a linear piecewise approximation solution over the two nodal element e , ($y_i \leq y \leq y_j$) where $u^{(e)} = [u_i \ u_j]$, $N = [N_i \ N_j]$ also u_i and u_j are the velocity component at the i^{th} and j^{th} nodes of the typical element (e) ($y_i \leq y \leq y_j$) furthermore, N_i and N_j are basis (or shape) functions defined as follows:

$$N_i = \frac{y_j - y}{y_j - y_i}, \quad N_j = \frac{y - y_i}{y_j - y_i}$$

Hence equation (3.8) takes the form

$$\int_{y_i}^{y_j} \begin{bmatrix} N_i' N_i' & N_i' N_j' \\ N_i' N_j' & N_j' N_j' \end{bmatrix} \begin{bmatrix} u_i \\ u_j \end{bmatrix} dy + \int_{y_i}^{y_j} \begin{bmatrix} N_i N_i & N_i N_j \\ N_i N_j & N_j N_j \end{bmatrix} \begin{bmatrix} \dot{u}_i \\ \dot{u}_j \end{bmatrix} dy + M_1 \int_{y_i}^{y_j} \begin{bmatrix} N_i N_i & N_i N_j \\ N_i N_j & N_j N_j \end{bmatrix} \begin{bmatrix} u_i \\ u_j \end{bmatrix} dy - P \int_{y_i}^{y_j} \begin{bmatrix} N_i \\ N_j \end{bmatrix} dy = 0$$

(14)

Simplifying equation (14) above we have;

$$\frac{1}{l} \begin{bmatrix} 1 & -1 \\ -1 & 1 \end{bmatrix} \begin{bmatrix} u_i \\ u_j \end{bmatrix} + \frac{l}{6} \begin{bmatrix} 2 & 1 \\ 1 & 2 \end{bmatrix} \begin{bmatrix} \dot{u}_i \\ \dot{u}_j \end{bmatrix} + \frac{M_1 l}{6} \begin{bmatrix} 2 & 1 \\ 1 & 2 \end{bmatrix} \begin{bmatrix} u_i \\ u_j \end{bmatrix} - \frac{lP}{2} \begin{bmatrix} 1 \\ 1 \end{bmatrix} = 0$$

(15)

Where $l = y_j - y_i = h$ and prime and dot denotes differentiation with respect to y and t respectively. Assembling the equations for the two consecutive elements $y_{i-1} \leq y \leq y_i$ and $y_i \leq y \leq y_{i+1}$ the following is obtained

$$\frac{1}{l^2} \begin{bmatrix} 1 & -1 & 0 \\ -1 & 2 & -1 \\ 0 & -1 & 1 \end{bmatrix} \begin{bmatrix} u_{i-1} \\ u_i \\ u_{i+1} \end{bmatrix} + \frac{1}{6} \begin{bmatrix} 2 & 1 & 0 \\ 1 & 4 & 1 \\ 0 & 1 & 2 \end{bmatrix} \begin{bmatrix} \dot{u}_{i-1} \\ \dot{u}_i \\ \dot{u}_{i+1} \end{bmatrix} + \frac{M}{6} \begin{bmatrix} 2 & 1 & 0 \\ 1 & 4 & 1 \\ 0 & 1 & 2 \end{bmatrix} \begin{bmatrix} u_{i-1} \\ u_i \\ u_{i+1} \end{bmatrix} - \frac{P}{2} \begin{bmatrix} 1 \\ 2 \\ 1 \end{bmatrix}$$

(16)

Considering the row corresponding to the node i to zero with $l = h$, from equation (16) the difference schemes reads

$$\frac{1}{h^2} (-u_{i-1} + 2u_i - u_{i+1}) + \frac{1}{6} (-\dot{u}_{i-1} + 4\dot{u}_i + \dot{u}_{i+1}) - \frac{M}{6} (u_{i-1} + 4u_i + u_{i+1}) = P$$

(17)

Using the trapezoidal rule on (17), the following system of equations in Crank-Nicolson method is obtained as

$$A_1 u_{i-1}^{n+1} + A_2 u_i^{n+1} + A_3 u_{i+1}^{n+1} = A_4 u_{i-1}^n + A_5 u_i^n + A_6 u_{i+1}^n + P^*$$

(18)

Where

Similarly by solving (7) and (8) using the same method we have

$$B_1 q_{i-1}^{n+1} + B_2 q_i^{n+1} + B_3 q_{i+1}^{n+1} = B_4 q_{i-1}^n + B_5 q_i^n + B_6 q_{i+1}^n + Q^*$$

(19)

$$C_1 \phi_{i-1}^{n+1} + C_2 \phi_i^{n+1} + C_3 \phi_{i+1}^{n+1} = C_4 \phi_{i-1}^n + C_5 \phi_i^n + C_6 \phi_{i+1}^n$$

(20)

Where

$$A_1 = 2 - 6r + rM_1 h^2, \quad A_2 = 8 + 12r + rM_1 h^2, \quad A_3 = 2 - 6r + rM_1 h^2$$

$$A_4 = 2 + 6r - rM_1 h^2, \quad A_5 = 8 - 12r - 4rrM_1 h^2, \quad A_6 = 2 + 6r - rM_1 h^2$$

$$B_1 = Pr - 3r, \quad B_2 = 4Pr + 6r, \quad B_3 = Pr - 3r, \quad B_4 = Pr + 3r, \quad B_5 = 4Pr - 6r, \quad B_6 = Pr + 3r$$

$$C_1 = Pr - 3r, \quad C_2 = 4Pr + 6r, \quad C_3 = Pr - 3r$$

$$C_4 = Pr + 3r, \quad C_5 = 4Pr - 6r, \quad C_6 = Pr + 3r$$

$$P^* = 12rh^2 (\theta_i^n + N\phi_i^n), \quad Q^* = 6r \text{Pr Ec} \left[\left[\frac{\partial u}{\partial y} \right]^2 + \frac{\partial^2 \phi}{\partial^2 y} \right]$$

Here $r = \frac{k}{h^2}$ and h and k are the mesh size along y direction and time direction respectively. Index i refers to space and j refers to the time. In equations (6), (7) and (8), taking $i = 1(1)n$ and using the initials and boundary conditions (9), the following system of equations is obtained

$$A_i X_i = B_i \quad i = 1(1)n$$

Where A_i matrices are of order n and X_i and B_i are column matrices having n components. The solution of the system of equations are obtained using Thomas algorithm for velocity, temperature and concentration. For various parameters the results are computed and presented graphically the skin friction, Nusselt number and Sherwood number are important physical parameters for this kind boundary layers flow. With known values of velocity, temperature and concentration fields,

The skin-friction at the plate is given by non-dimensional form

$$\tau = \left[\frac{\partial u}{\partial y} \right]_{y=0, y=1}$$

(21)

The rate of heat transfer coefficient can be obtained in the terms of Nusselt number in non-dimensional form, given as

$$Nu = - \left[\frac{\partial \theta}{\partial y} \right]_{y=0, y=1}$$

(22)

The rate of mass transfer coefficient can be obtained in terms of Sherwood number in non-dimensional form given by

$$Sh = - \left[\frac{\partial \phi}{\partial y} \right]_{y=0, y=1}$$

(23)

3. Results and Discussion

The current extended model was solve using finite element method .I n the numerical calculations arbitrary values were chosen for magnetic parameter (M), the Dufour number (Df), the Eckert number (Ec) the Schmidt number (Sc), the Ratio of mass transformation (N), the porosity parameter (K), the Buoyancy parameter (r_i) unless otherwise while Prandtl number ($Pr = 0.71, Pr = 3, Pr = 7$) which physically represent air and water respectively. Its interested to report that the all the profiles (2 to 21) in the present work were intensified due to presence of Dufour number (Df) and, buoyancy parameter (r_i) in comparison with work of Prabhakar [15].

3.1 Velocity Profiles

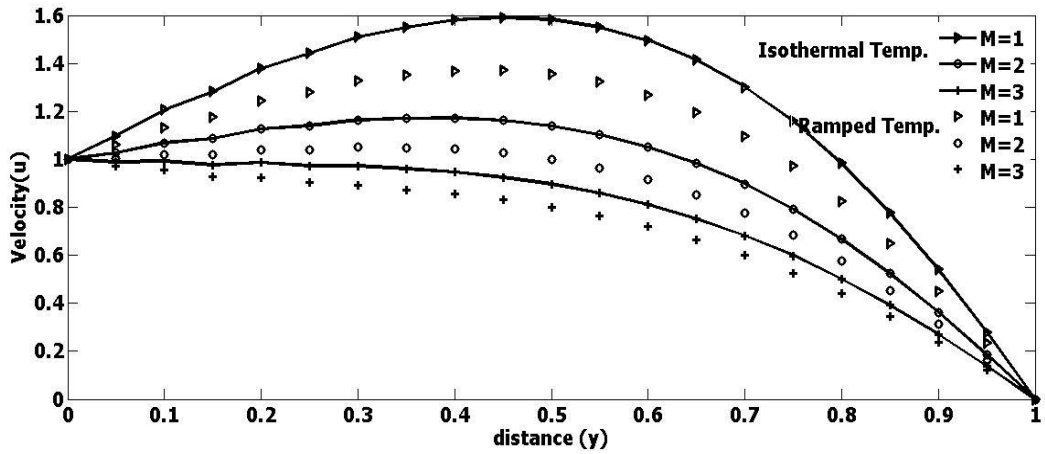


Figure 2: Effect of M on velocity profile

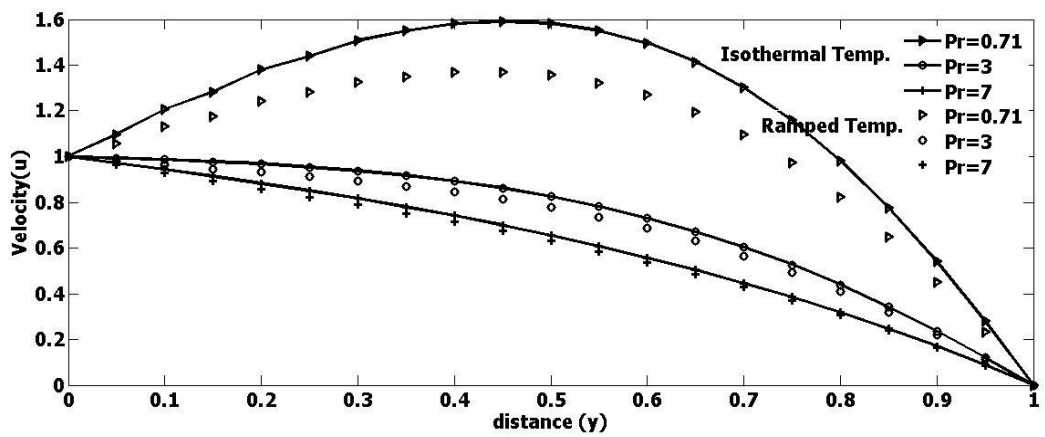
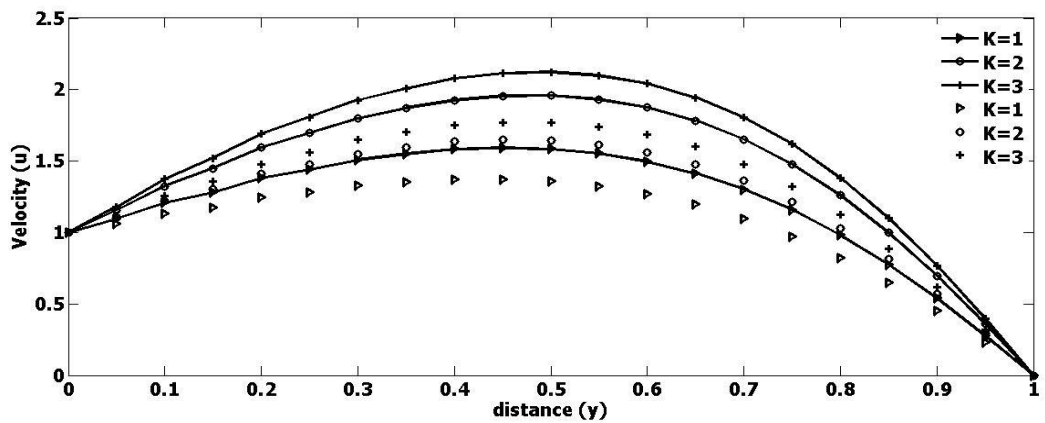


Figure 3: Effect Pr on velocity profile



Effect 4: of K on velocity profile

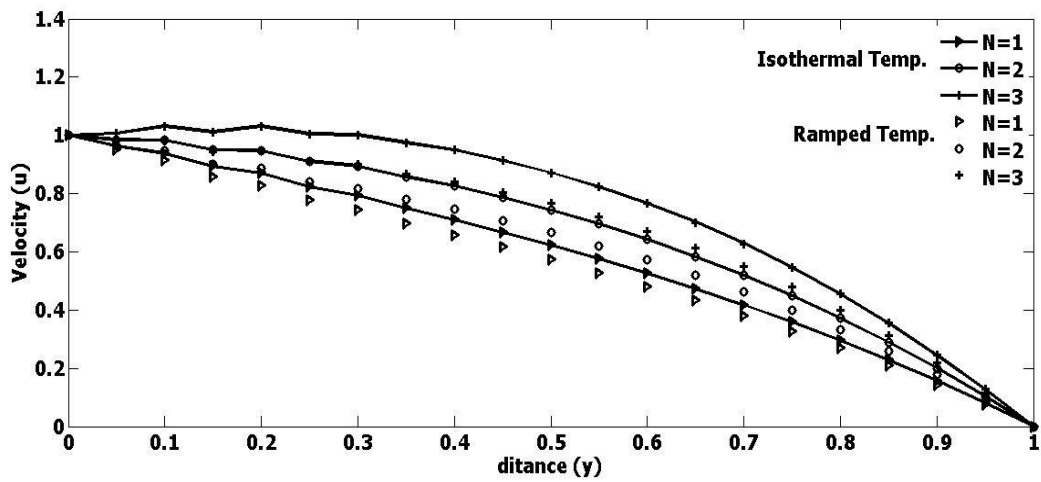


Figure 5: Effect of N on velocity profile

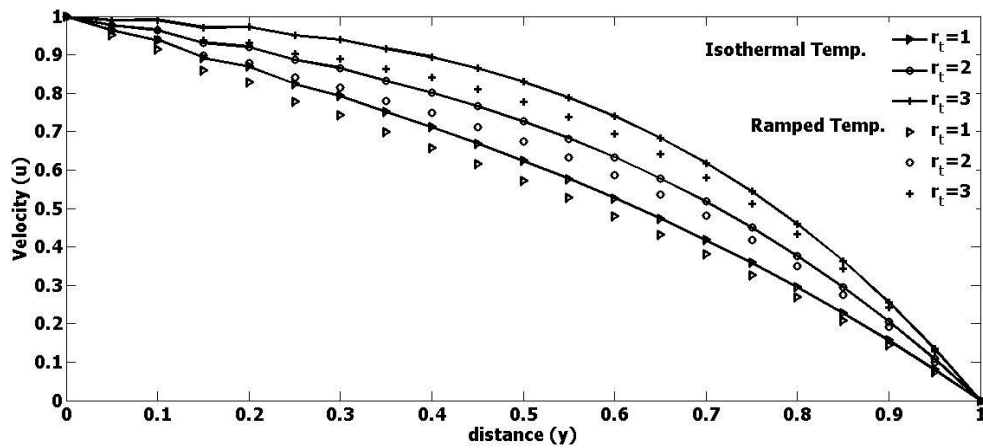


Figure 6: Effect r_t on velocity profile

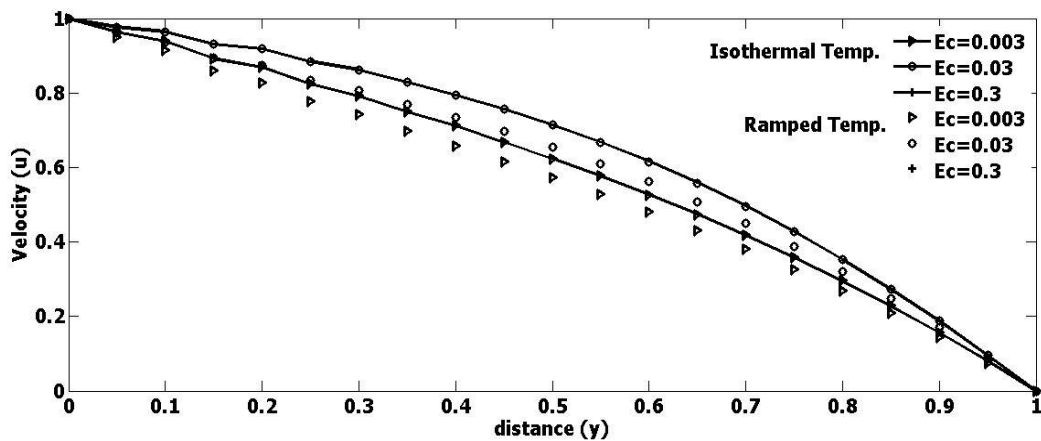


Figure 7: Effect of Ec on velocity profile

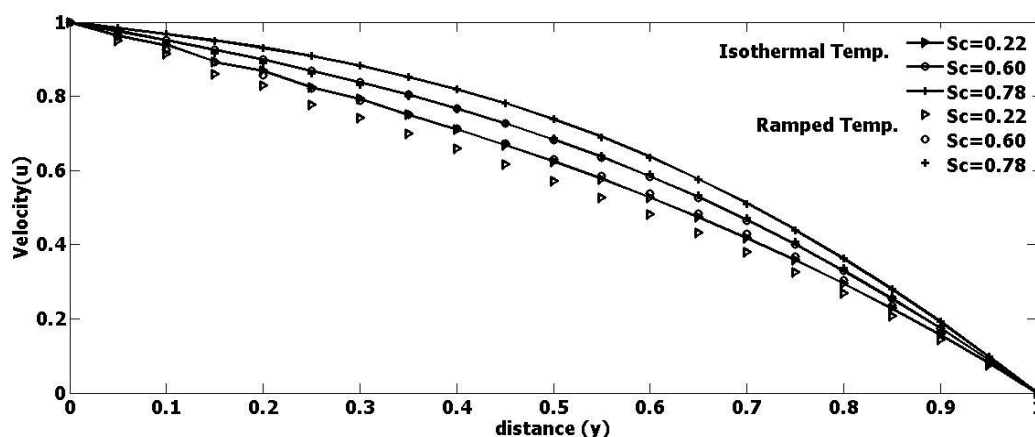


Figure 8: Effect of Sc on velocity profile

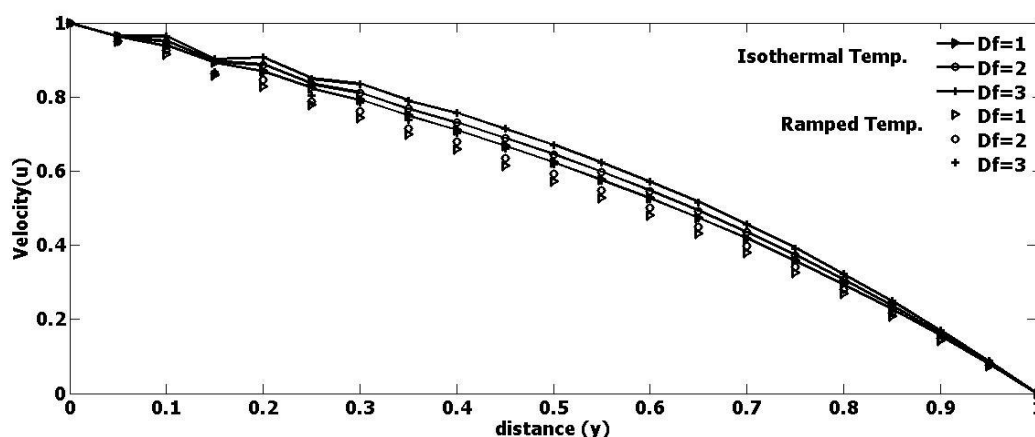


Figure 9: Effect Df on velocity profile

Figure 2 illustrates the behavior of velocity for different values of Magnetic parameter M for both isothermal and ramped plate. From that figure it is noticed that as Magnetic parameter M increase the fluid velocity gets reduced at all point of the flow field. This is true since magnetic parameter produce resistive force, which acts opposite direction to the fluid motion. Similarly figure 3 displays the control Prandtl number Pr on fluid velocity for both isothermal and ramped plate. From that figure it is revealed that as Prandtl number Pr rises the fluid velocity also diminishes at all point of the flow field.

Figure 4 shows the effect control of porosity parameter K on fluid velocity for both isothermal and ramped plate and it is also observed that an increase porosity parameter K leads to raise in fluid velocity at all point of the flow. Similarly figure 5 demonstrates the influence of the ratio of mass transfer parameter N on the fluid velocity for both isothermal and ramped plate. It is shown that the fluid velocity gets enhanced by increasing the values of the ratio of mass transfer parameter N for both isothermal and ramped plate. Likewise figure 6 demonstrate the influence of buoyancy term r_t on the fluid velocity for both isothermal and ramped plate. It is also clearly observed that the fluid velocity significantly get enhanced to for both isothermal and ramped plate by rising the values of buoyancy term r_t .

Figure 7 displays the effect of Eckert number Ec on the fluid velocity for both isothermal and ramped plate. It is observed that the fluid velocity slightly gets enhanced by increasing the values of Eckert number Ec increases the fluid velocity for both isothermal and ramped plate. Similarly figure 8

displays the effect of Schmidt number Sc on the fluid velocity for both isothermal and ramped plate. It is seen that the fluid velocity slightly gets enlarged by increasing the values of Schmidt number Sc for both isothermal and ramped plate. In a similar way figure 9 displays the effect of Dufour number Df on the fluid velocity for both isothermal and ramped plate. It is also observed that increasing the values of Dufour number Df leads to slight raise in the fluid velocity for both isothermal and ramped plate.

3.2 Temperature Profiles

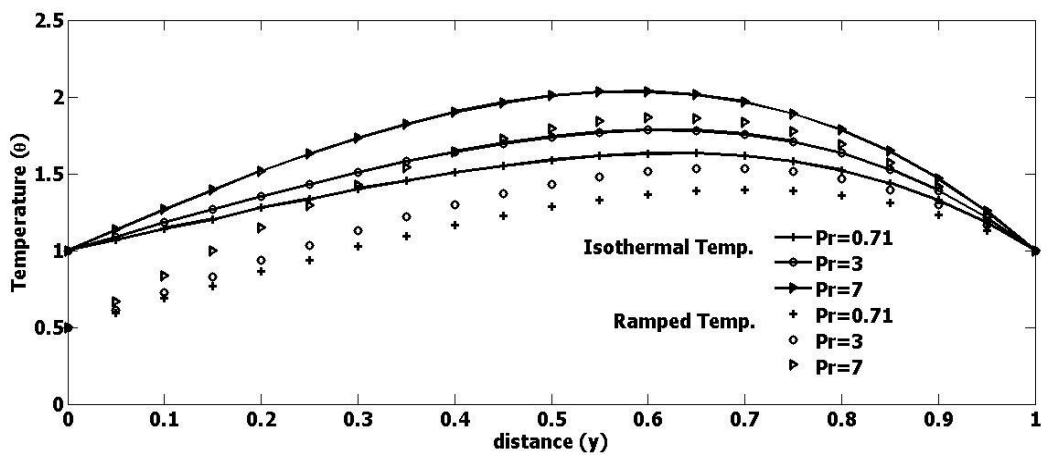


Figure 10: Effect Pr on temperature profile

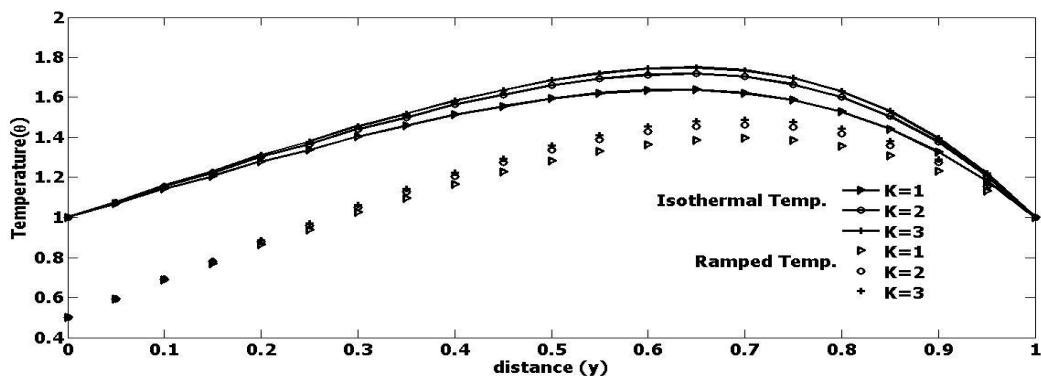


Figure 11: Effect of K on temperature profile

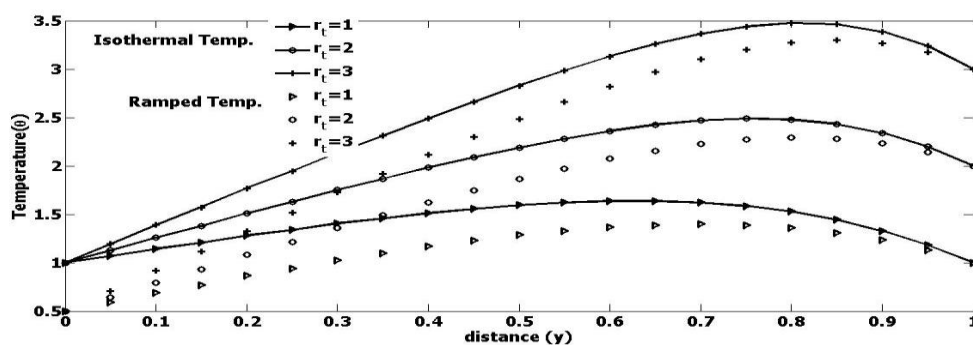


Figure 12: Effect r_t on temperature profile

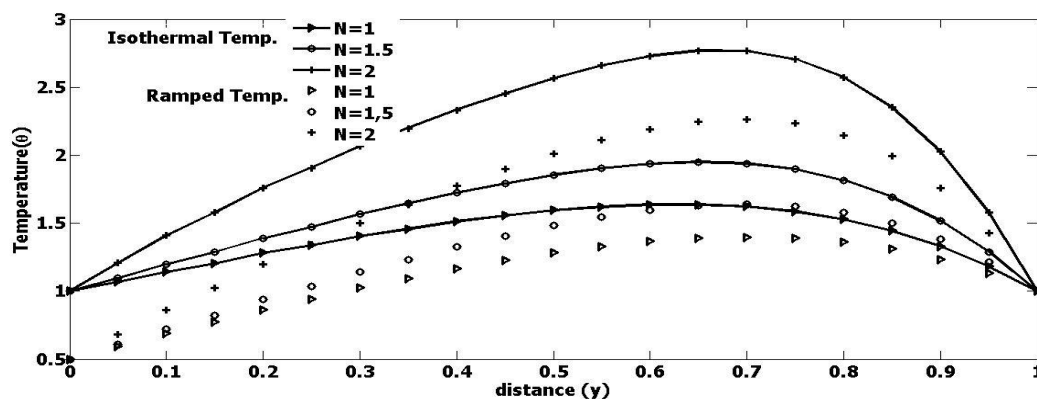


Figure 13: Effect N on temperature profile

Figure 10 depicts the influence of Prandtl number Pr on fluid temperature for both isothermal and ramped plate. It is revealed from that figure the fluid temperature gets reduced by increasing the values of Prandtl number Pr . While figure 11 depicts the influence of porosity parameter K on fluid temperature for both isothermal and ramped plate. It is also revealed from the figure that figure the fluid temperature increases by increasing the values of porosity parameter K . Similarly figure 12 depicts the effect of buoyancy effect parameter r_t on fluid temperature for both isothermal and ramped plate. It is clearly seen from that figure the fluid temperature gets intensified by increasing the values of buoyancy effect term r_t . In a similar way figure 13 shows the effect of ratio of mass transfer parameter N on fluid temperature for both isothermal and ramped plate. It is also clearly seen from that figure the fluid temperature gets significantly boosted by increasing the values of ratio of mass transfer parameter N for both isothermal and ramped plate.

3.3 Concentration Profile

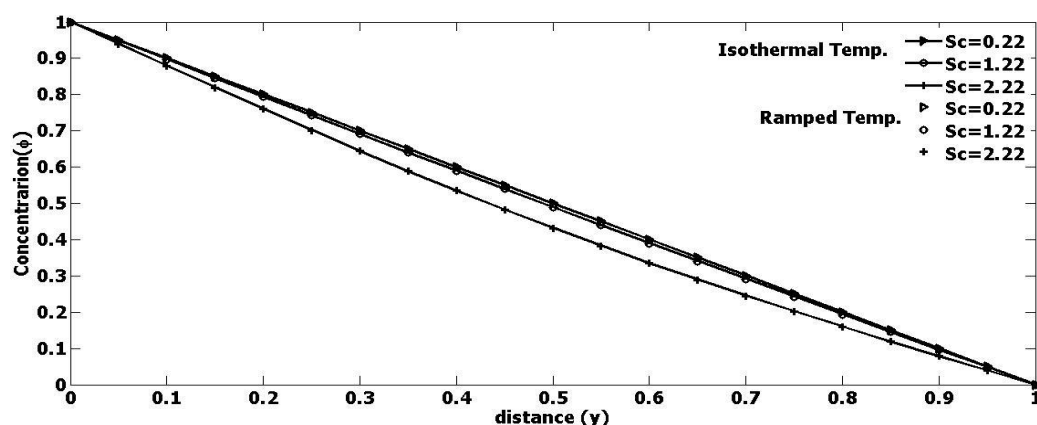


Figure 14: Effect Sc on Concentration profile

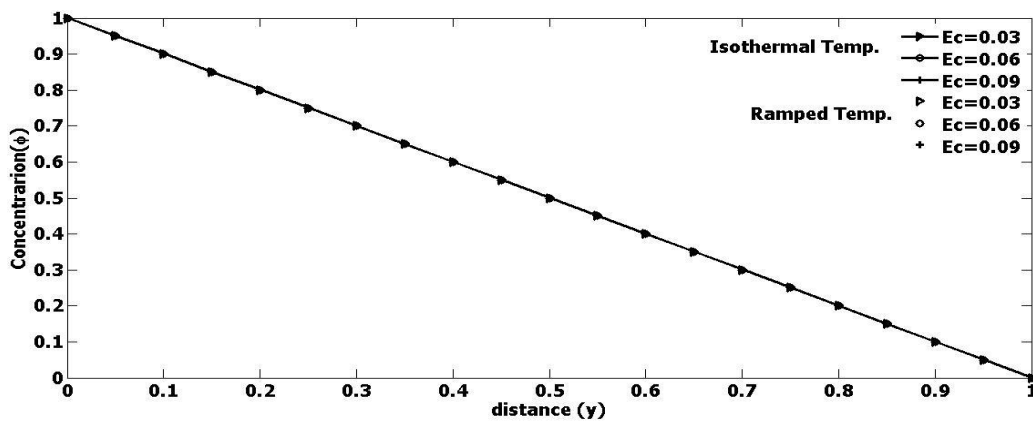


Figure 15: Effect of Ec on Concentration profile

Figure 14 and figure 15 displays the effect of Schmidt number Sc and Eckert number Ec on the fluid concentration for both isothermal and ramped plate. It is seen that the fluid concentration does not decrease or increase by increasing Schmidt number Sc or Eckert.

3.4 Skin Friction Profile

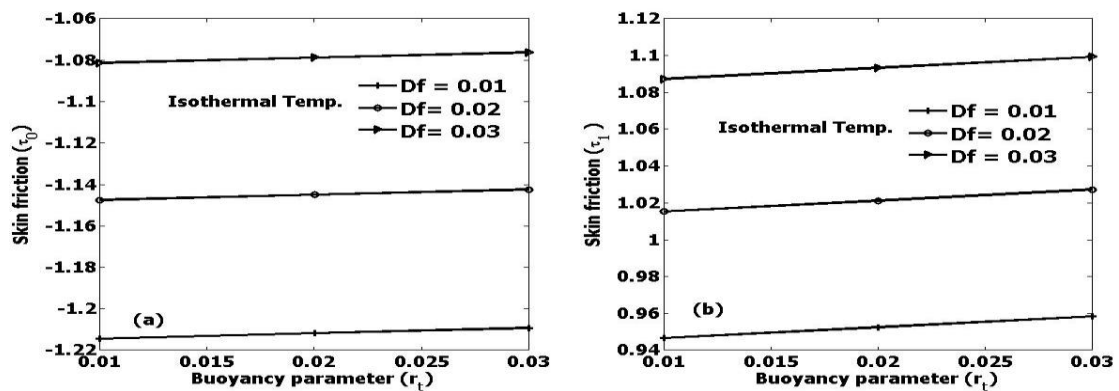


Figure 16: Effect of Df and r_t on skin friction due to isothermal temperature

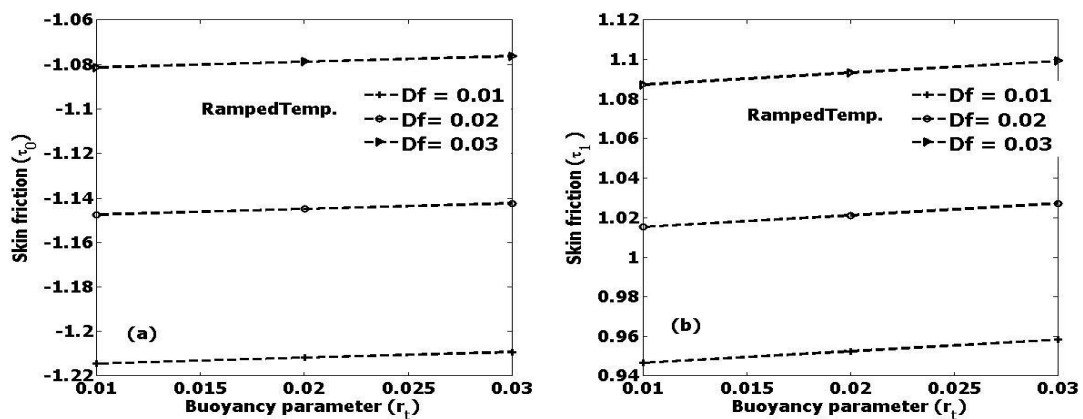


Figure 17: Effect of Df and r_t on skin friction due to ramped temperature

Figure 16 and 17 display the Dufour number Df and buoyancy parameter r_t on the fluid skin friction for both isothermal and ramped temperature and it is clearly seen in both figures that skin friction in figures (a) and (b) gets significantly enhanced with increase Dufour number Df and slightly enhanced with increasing buoyancy parameter r_t .

3.5 Nusselt Number

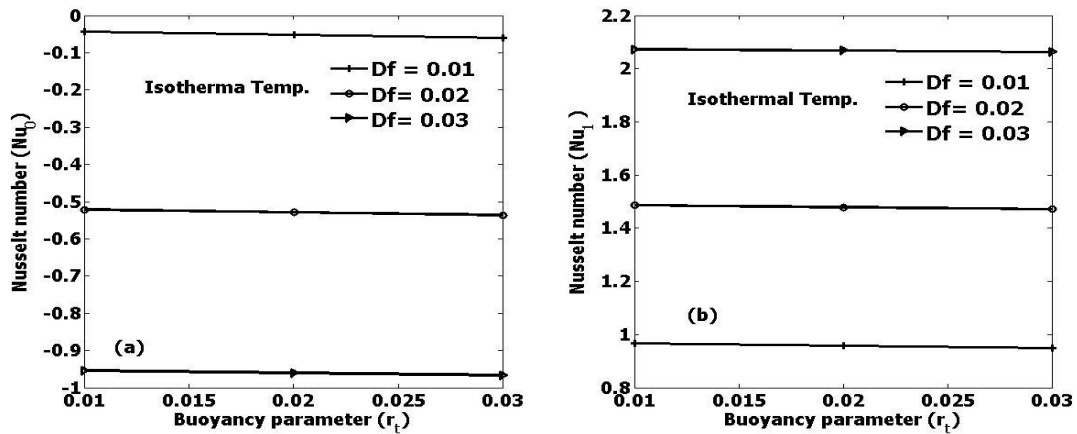


Figure 18: Effect of Df and r_t on Nusselt number due to isothermal temperature

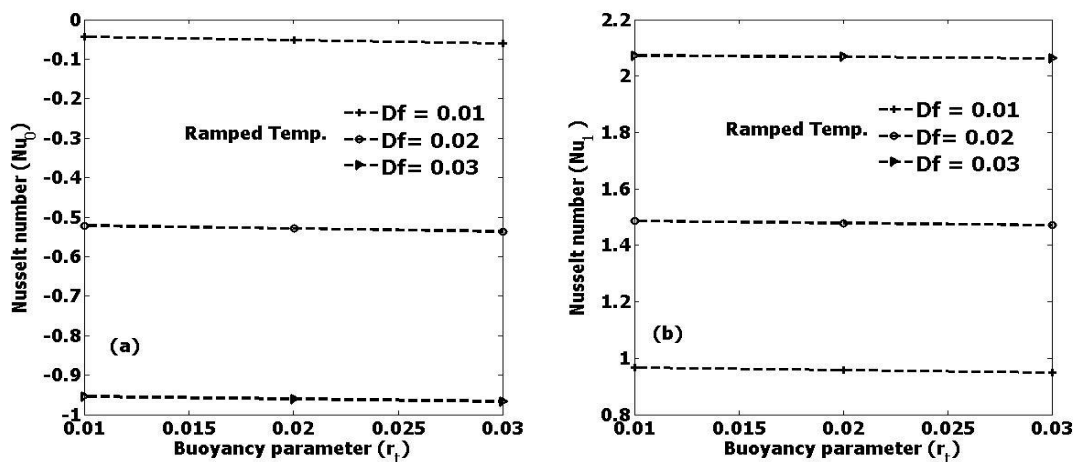


Figure 19: Effect of Df and r_t on Nusselt number due to ramped temperature

Figure 18 and 19 display the effect of Dufour number Df and buoyancy parameter r_t on fluid Nusselt number for both isothermal and ramped temperature and it is clearly seen that the Nusselt number in figures 18 and 19 (a) gets reduced by increasing Dufour number Df and it slightly increase by increasing buoyancy parameter r_t . While in figures 18 and 19(b), fluid Nusselt number gets intensified with increase Dufour number Df and there is no noticeable increase or decrease by increasing buoyancy parameter r_t .

3.6 Sherwood Number

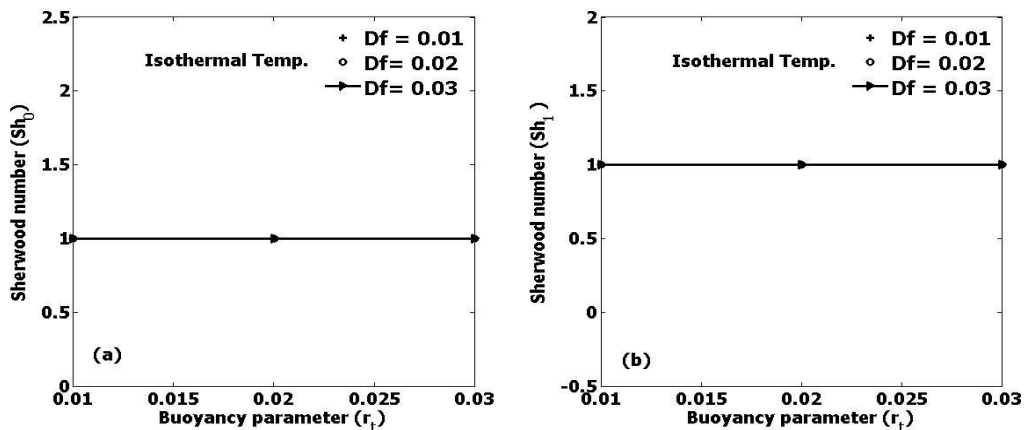


Figure 20: Effect of Df and r_t on Sherwood number due to isothermal temperature

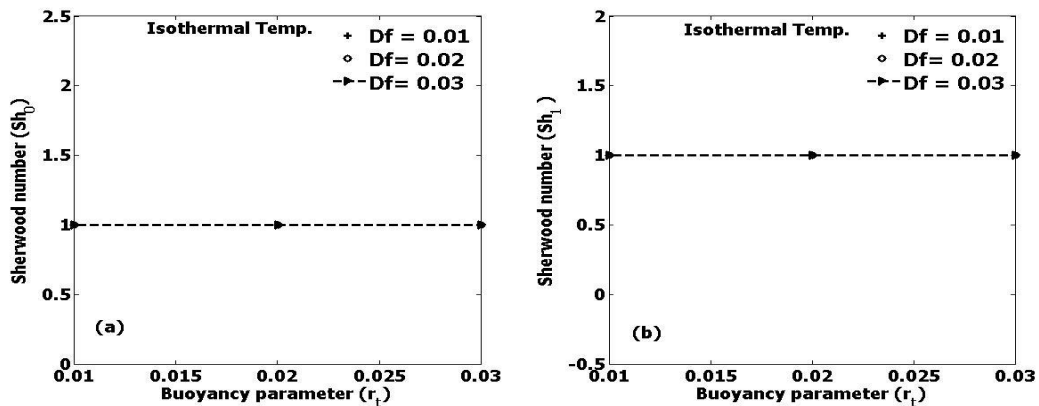


Figure 21: Effect of Df and r_t on Sherwood number due to ramped temperature

Figure 20 and figure 21 displays the effect of Dufour number Df and buoyancy parameter r_t on fluid Sherwood number for both isothermal and ramped temperature and it is clearly seen that there is no any noticeable increase or decrease in Sherwood number in both figures by increasing either Dufour number Df or buoyancy parameter r_t .

4. Conclusion

The Dufour effects of electrically conductive fluid of unsteady heat and mass transfer Couette in the presence of buoyancy distribution effects due to ramped and isothermal temperature was investigated. From the study, the following conclusions were drawn:

- i. The velocity profile gets enlarged with increase of Dufour number Df , porosity parameter K , ratio of mass transfer parameter N , buoyancy effect term parameter r_t Eckert number Ec , Schmidt number Sc and decreases with increase of Magnetic parameter M , Prandtl number Pr for both ramped and Isothermal temperature
- ii. The temperature profile gets magnified with increase of Porosity parameter K , ratio of mass transfer parameter N , buoyancy effect term parameter r_t and decreases with the increase of Prandtl number Pr for both ramped and Isothermal temperature

- iii. The concentration profile gets enhanced slightly with increase of Schmidt number Sc and it neither increase nor decrease with increase of Eckert number Ec for both ramped and Isothermal temperature
- iv. At both $y=0$ and $y=1$, the skin friction is significantly enhanced with increase of Dufour number Df and slightly increase with increase of buoyancy parameter r_t
- v. At $y=0$ the Nusselt number decreases with increase of Dufour number Df and slightly increase with increase of buoyancy parameter r_t . At $y=1$ the Nusselt number gets enhanced with increase of Dufour number Df and there is no noticeable increase or decrease with increase of buoyancy parameter r_t
- vi. At both $y=0$ and $y=1$, there is no noticeable increase or decrease in Sherwood number with increase of Dufour number Df and buoyancy parameter r_t .

References

- [1] Siva, R. S., Ali, J. C. and Anjan, K. S. (2016). Heat and Mass Transfer Effects on MHD Natural Convection Flow Past an Impulsively Moving Vertical Plate with Ramped Temperature. *American Journal of Heat and Mass Transfer* 3 (2016), 129-148
- [2] Shankar, B. G. & Rajashekar, M. N. (2017), Finite Element Solution On Effects Of Viscous Dissipation & Diffusion Thermo On Unsteady MHD Flow Past An Impulsively Started Inclined Oscillating Plate With Mass Diffusion & Variable Temperature. *International Research Journal of Engineering and Technology*; 4 (2), 471-477
- [3] Rajakumar, K. V. B., Balamurugan, K. S., Umasankara, R. M. & Ramana, V. (2018). Radiation, Dissipation and Dufour Effects on MHD Free Convection Casson Fluid Flow through a Vertical Oscillatory Porous Plate with Ion-Slip Current. *International Journal of Heat and Mass Transfer Technology*; 36 (2), 494-508.
- [4] Chandra P. R., Raju M. C. & Raju, G. S. S. (2018). Magneto Hydrodynamic Convective Double Diffusive Laminar Boundary Layer Flow Past an Accelerated Vertical Plate. *International Journal of Engineering Research in Africa*; 20, 80-92.
- [5] Reddy, G. J., Raju, R. S., Rao, J. A. & Gorla, R. S. R. (2017). Unsteady MHD Heat Transfer in Couette Flow of Water at 4°C in a Rotating System with Ramped Temperature via Finite Element Method. *International Journal of Applied Mechanics and Engineering*; 22(1), 145-161.
- [6] Bilal, M. A., Hayat, T., Alsaedi, A., Shehzad, A.S. (2016). Soret and Dufour effects on the mixed convection flow of an Oldroyd-B fluid with convective boundary conditions. *Elsevier Journal*, 6 (2016), 917–924.
- [7] Emmanuel, M. A., Yakubu, I. S., Daniel, G. A. (2015). Analytical Solution of Dufour and Soret Effects on Hydromagnetic Flow Past a Vertical Plate Embedded in a Porous Medium. *Advances in Physics Theories and Applications*, 44 (2015) 2225-0638.
- [9] Gbadeyan, J.A., Oyekunle, T.L., Fasogbon, P.F., and Abubakar, J.U. (2018). Soret and Dufour effects on heat and mass transfer in chemically reacting MHD flow through a wavy channel. *Journal Of Taibah University For Science*, 5(12) 631–651.
- [10] Falodun, B.O and Idowu, A.S., (2019). Soret–Dufour effects on MHD heat and mass transfer of Walter’s-B viscoelastic fluid over a semi-infinite vertical plate: spectral relaxation analysis. *Journal of Taibah University for Science*. 13(1) 49-62.
- [11] Reddy, S.S., Vijayabhaskar, C. & Mahendar, D. (2018). Unsteady MHD Flow over an Inclined Porous Plate Embedded in Porous Medium with Heat Absorption and Soret-Dufour Effects. *International Journal of Pure and Applied Mathematics*; 120 (6), 8021-8049.
- [12] Shagaiya, D. S. & Daniel, S. K. (2015). Effects of Buoyancy and Thermal Radiation on MHD Flow over a Stretching Porous Sheet using Homotopy Analysis Method. *Alexandria Engineering Journal*; 54, 705-712.
- [13] Shagaiya, Y. D. & Simon, K. D. (2015). Effects of buoyancy and thermal radiation on MHD flow over a stretching porous sheet using homotopy analysis method. *Alexandria Engineering Journal*, 54 (2015), 705-712.
- [14] Adamu, G. C., and Bandari, S. (2018). Buoyancy Effects on MHD Flow of a Nanofluid over a Stretching Sheet with Chemical Reaction. *International Journal of Innovative Research in Science, Engineering and Technology*, 7 (11), 2319-8753
- [15] Prabhakar Reddy, B. (2016). Mass Transfer Effects on an Unsteady MHD Free Convective Flow of an Incompressible Viscous Dissipative Fluid Past an Infinite Vertical Porous Plate. *International Journal of Applied Mechanics and Engineering*, <https://doi:10.1515/ijame-2016-0009>